

New approach to brake pad wear modelling based on test stand friction-mechanical investigations

Indexed by:



Wojciech Sawczuk^a, Agnieszka Merkisz-Guranowska^a, Armando-Miguel Rilo Cañás^b, Sławomir Kołodziejcki^c

^aPoznan University of Technology, Institute of Transport, ul. Piotrowo 3, 60-965 Poznań, Poland

^bPoznan University of Technology, PhD studies, ul. Piotrowo 3, 60-965 Poznań, Poland

^cAKSA Poland Hydraulics ul. Unii Lubelskiej 1, 61-249 Poznań, Poland

Highlights


- The multiple regression is applied for modelling of brake pad mass wear.
- The speed and the mass have the greatest impact on the brake pad wear.
- contact surface, thickness and clamping pads against the disc do not influence the mass wear of the pads.
- brake pads in a disc brake system do not wear evenly despite its symmetric lever system.

Abstract

The paper presents the results of investigations of a railway disc brake system related to the mass wear of its brake pads. The tests were carried out on a certified brake stand designed to determine the friction-mechanical characteristics of the brakes. The test stand was additionally equipped with a thermographic camera to observe the contact points of the brake pads with the disc. Particular attention was drawn to investigating the impact on the mass wear of the brake pads of such parameters of the braking process as contact surface of the brake pad with the rotor, thickness of the brake pads as the indicator of their initial wear, clamping force of the pads against the rotor, rail vehicle mass to be decelerated, and speed, at which the deceleration begins. The scientific aim of the paper is to present the relations between the mass wear of the brake pads and the quantities that characterize the braking process. A regression model was determined to estimate the wear of the brake pads based on a single braking process with the preset input quantities.

Keywords

brake pad mass wear, test stand disc brake investigations, rail vehicle disc brake.

This is an open access article under the CC BY license (<https://creativecommons.org/licenses/by/4.0/>) 

1. Introduction

Emissions from road traffic, in particular, are a major contributor to ambient dust concentrations. These emissions are targeted at increasingly stringent European emission standards [33]. These legal restrictions make it possible to reduce exhaust emissions, e.g. from internal combustion engines of cars. However, environmentalists also point to emissions from brake wear or tire wear, which in the form of wear products pollute the environment and are components of dust and gases in the air. The research by Glišović et al. [14] shows that the braking system, in particular friction disc brakes of motor vehicles or railroads, also causes pollution of the environment due to dusting in the form of particulate matter (PM) of wear products, which has an impact on environmental pollution and deterioration of the health of people staying in the vicinity of vehicles (cars or trains). These are elements such as antimony and copper in brake shoes, which are considered to be highly harmful. The emission of particulate matter (PM) from the braking system depends on the physical and chemical properties of the friction material and the number of brakes. In rail vehicle friction brakes, the most significant in the minds of design

engineers, manufacturers, and researchers is the assurance of friction characteristics on the level compliant with the UIC or EN-PN requirements [42, 43]. This is very important in terms of brake efficiency, that is, the braking distance, which is the key factor in ensuring that the vehicle stop is successfully in any weather conditions and regardless of the condition of the railway infrastructure. The characteristics of friction material wear are determined in test stand investigations. In their laboratories, for example, Knorr-Bremse in Munich and Lumag in Budzyn, manufacturers of brake pads select such a composition of the friction material as to obtain a compromise between friction-mechanical characteristics and wear. Recently, environmental aspects have also been taken into account. The first action in this matter was the elimination of asbestos from friction materials due to its carcinogenic nature (as confirmed in the 1970s of the last century [5, 6]), although, in connection with the copper fibers, it forms the best friction material in terms of resistance to high temperatures and stability [7, 28]. Since then, engineers have been searching for new materials that would replace asbestos while maintaining its friction characteristics [2]. Research is being conducted on the influence of asbestos-free particle size in the range of 125-710 µm on brake pad wear [3,

E-mail addresses: W. Sawczuk (ORCID: 0000-0002-5049-6644): wojciech.sawczuk@put.poznan.pl, A. Merkisz-Guranowska (ORCID: 0000-0003-2039-1806): agnieszka.merkisz-guranowska@put.poznan.pl, A-M. Rilo Cañás (ORCID: 0000-0003-2033-5070): armando.rilocanas@doctorate.put.poznan.pl, S. Kołodziejcki (ORCID: 0000-0003-1254-5043): slawomir.kolodziejcki@aksapoland.pl

49]. The environmental emission of the friction products generated by brake systems was a subject of many works [4, 14]. Attention was drawn to questions related to environment pollution as well as the impact of wear products on human health [30], including airborne particles [27, 47] and solid particles that are particularly toxic to humans and animals [25, 26]. Furthermore, used brake pads, regardless of the intensity of wear, in the form of a steel plate and the remaining friction material as waste, are subject to disposal [46]. To reduce the said impacts, additional actions were initiated to eliminate or reducing the use of copper in the production of friction materials [22, 25]. Many scientific centers have attempted to replace toxic and hazardous components with new organic materials based on modified phenolic and epoxy resins [3, 16], basalt and glass fibers [20], low-content copper fibers, for example 7% [40, 51], fibers with palm and other kernels [30], asbestos-free cane ash sugar as filler [8] or such components as titanium [41]. There have also been successful attempts to use banana peel waste to replace asbestos and traditional phenolic and phenol-formaldehyde resins [18]. The frictional characteristics of traditional brake pads indicate that banana peels can be a substitute for asbestos in the production of pads. In addition, the friction line wear issues on steel discs with various alloy additives described in [9]. In the area of novel friction materials, tribological investigations are underway related to the determination of their friction-mechanical characteristics, investigating their potential for long-life applications in varied braking conditions such as heavy rainfall and moisture [11] without the adverse impact on the natural environment [21, 29, 48]. An important problem discussed in [19] is not only the environmental impact of the particulate matter and volatile particles generated during braking but also their impact on the brake system itself and the friction characteristics related to its efficiency. These investigations also address the requirements in terms of vibration and noise generated by the brake systems described in [22]. In [34, 35], the authors also indicate the relations between the mass wear of the brake pads and the vibroacoustic signal generated by the disc brakes. All the addressed problems require knowledge of the mechanism of friction and wear of the friction materials described in [1, 12, 24], which papers, in addition to models of friction and wear, also rely on stationary tests performed under test stand and actual operating conditions [39]. Other researchers [17, 38, 50] have presented results of FEM numerical simulations of brake pads for different friction materials using Archard and Euler wear equations. The wear of the brake friction components in railway vehicles is particularly important for the owners of the rolling stock for whom the purchase of friction materials is a significant operational cost. In the case of electric trains or electric locomotives, the wear of friction pads can be reduced owing to the nature of operation of their brake systems. In these vehicles, most of the braking power comes from the electrodynamic (frictionless) brake, utilizing electric motors as generators that provide additional force. Only in the final phase of braking, due to the characteristics of the electric motor, is the insufficient braking force supplemented with the friction brake. The share of the electrodynamic brake compared to the friction one is approximately 80/20%. In this area [32, 45], many research centers conduct their research on the continuous increase in the efficiency of electrodynamic brakes. This applies to the storage of braking energy in new technology for example CLAB or supercapacitors [10], the installation of wind turbines along railway tracks to supply traction [31], the creation of new train schedules to reduce the use of brakes or to increase the efficiency of the recuperation process [44]. The use of electrodynamic brakes significantly reduces the emission of particles and gases generated by friction brakes, which significantly reduces the mass wear of the

brake pads in pneumatic or electro-pneumatic brake systems. The authors, based on their research, present the results of the quantitative wear of the friction material in the form of particulate matter (PM) from a single braking with different braking process configurations (speed, pressure, or mass to decelerate). On this basis, an attempt was made to model the weight consumption of the brake pad. The model presented in the article applies to particulate matter (PM) due to measurement of the weight wear of the friction material. The developed model of friction pad wear, e.g. for constructors of the braking system or railway carriers, with known speed limits on the route, will allow one to calculate the weight consumption of friction materials emitted to the natural environment.

In further works of the authors, it is planned to expand the model of weight wear of friction pads with new variables. Many disc brake system designs feature perforated or split brake discs. These are solutions that improve assembly or heat exchange. However, they increase the wear of the friction pads.

3. Research object and methodology

The investigations of the mass wear of the brake pads were carried out on a certified inertia brake test stand located at ukasiewicz Poznanski Institute of Technological Sciences (Poznan Technological Institute). The test stand for railway disc brakes is shown in Fig. 1. This test stand allows performing friction-mechanical tests of rail vehicle pads brakes and disc brakes under conditions reflecting the actual operating ones when decelerating a rail vehicle. During these investigations, the authors additionally applied a Flir e60 thermographic camera to monitor the temperature distribution on the brake pads after braking.

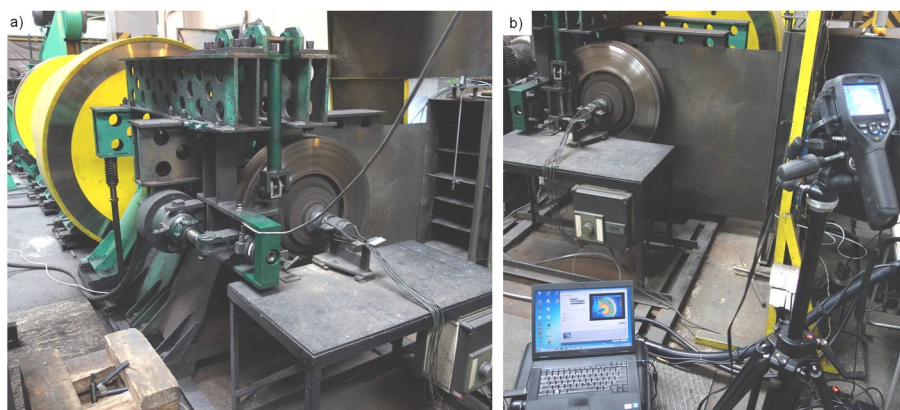


Fig. 1. The test stand for railway disc brakes: a) view on the operational part of the test stand with the rotating masses, b) view of the investigated disc and the thermographic camera.

The investigations were carried out according to the principle of active experiment according to the methodology described in the articles of Gowacz et al., Rymaniak et al. and Sawczuk et al. [15, 33, 37]. Throughout the investigations, the input parameters were purposefully modified (the initial parameters of the braking process) and their influence on the change of the output parameters (mass wear of the brake pads) was observed. The investigations were carried out on organic brake pads type 175 and 200 (Fig. 2) mating with a ventilated brake disc of 640×110 in size made of grey cast iron. Figures 2, c) and Figure 2, d) present the view of the reverse side of the brake pads with the fitting elements. Apart from the area of the contact surface (175 or 200 denotes the contact surface area with the disc in cm²), a significant difference among the brake pads is the length of the guiding elements on the reverse side of the pad to be fitted to the holders.

A single set of brake pads includes 4 type 175 or 200 pads. FR20H.2 pads, according to the manufacturer's procedure and the requirements indicated in UIC Code 541-3 [42], were made from a thermosetting resin, synthetic elastomer, metal and organic fiber, and friction modifi-

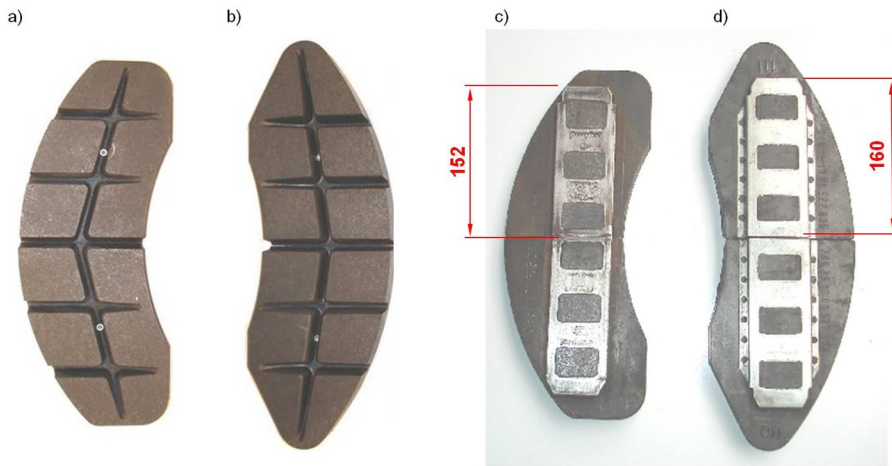


Fig. 2. Brake pads used in the investigations: a) type 175 – view from the disc contact side, b) type 200 view from the disc contact side, c) type 175 view from the reverse side, d) type 200 view from the reverse side

ers. During the tests on the test stand, two types of pads, three sets each of different thicknesses (indicating their initial wear). The first set were new pads of the thickness of 35 mm, the second and the third were pads worn to the thickness of up to 25 and 15 mm, accordingly.

The investigations were carried out according to the UIC 541-3 [42] chart in terms of the selection of the pad clamp force and the mass to be decelerated per one brake disc [42]. Parameters modified during the tests were: thickness of the brake pads, speed at which the braking was initiated ($v = 50, 80, 120, 160$ and 200 km/h), the clamping force of the pad against the disc ($N = 16, 25, 26, 28, 36, 40$ and 44 kN) and the mass to be decelerated per single brake disc ($M = 4.4, 4.7, 5.7, 6.7$ and 7.5 t).

Before the initiation of the actual tests, a series of braking was performed to run-in the pads. According to [42], preliminary braking is to continue until the brake pads are worn on more than 75% of the surface. After each braking, the pads of a given thickness, preset speed, clamping force, and mass to be decelerated were weighed on an electronic scale of the accuracy of 1 gram. During the friction-mechanical tests, the authors carried out 150 instances of braking excluding the braking related to the running-in of the pads.

4. Test results and analysis

During tests stand investigations, attempts were made to determine the relation of the mass wear of parameters the pads as a function of such as brake pad contact surface area with the disc, initial speed of deceleration, clamping force of the pads against the brake disc and the mass to be decelerated per single brake disc. In the first place, for different combinations of the clamping force and pad thickness, the authors determined and validated the mass wear increment of the pads as a function of the running speed, at which the deceleration was initiated. Table 1 contains selected results for the measurement of mass wear (in grams) of the pads for one of the selected combinations.

When analyzing the results presented in Table 1, the authors have concluded that the mass wear of the pads increases along with the initial

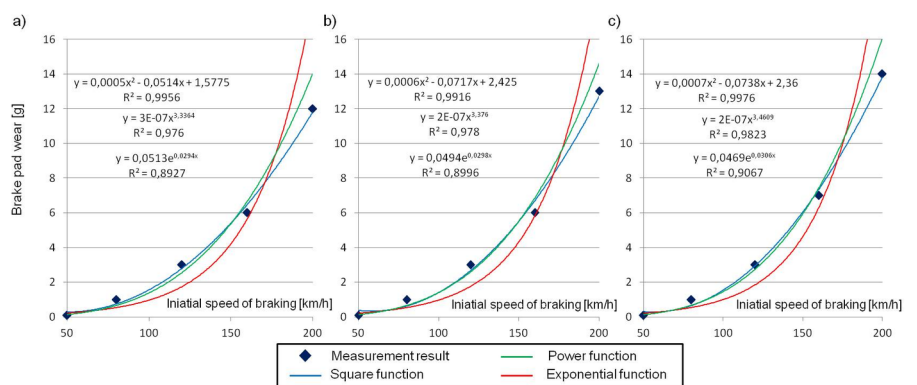


Fig. 3. The relationship of brake pad wear as a function of initial speed at $N=40$ kN and $M_h=6.7$ t, braking with: a) new 35 mm brake pads, b) 25 mm brake pads, c) 15 mm brake pads

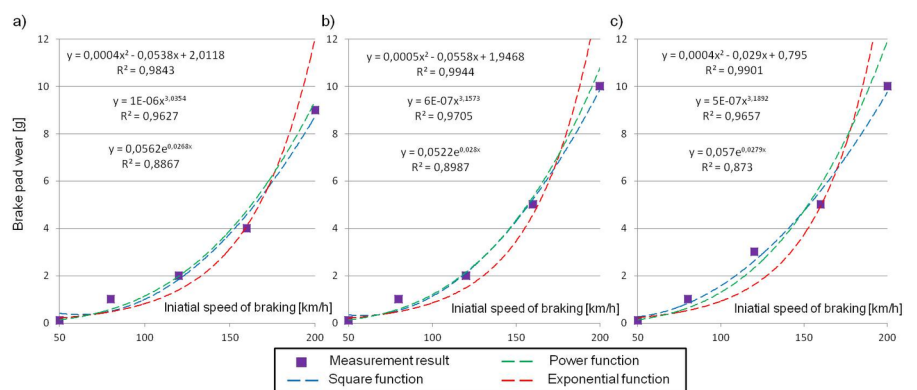


Fig. 4. The relationship of brake pad wear as a function of initial speed at $N=28$ kN and $M_h=6.7$ t, braking with: a) new 35 mm brake pads, b) 25 mm brake pads, c) 15 mm brake pads

Table 1. Mass wear (in grams) of the brake pads after braking to a complete stop

Force $N=28$ kN, mass to be decelerated $M_h=6.7$ t				Force $N=40$ kN, mass to be decelerated $M_h=6.7$ t			
Initial speed of deceleration, km/h	Pad thickness			Initial speed of deceleration, km/h	Pad thickness		
	$G_1=35$ mm	$G_2=25$ mm	$G_3=15$ mm		$G_1=35$ mm	$G_2=25$ mm	$G_3=15$ mm
50	0	0	0	50	0	0	0
80	1	1	1	80	1	1	1
120	2	2	3	120	3	3	3
160	4	5	5	160	6	6	7
200	9	10	10	200	12	13	14

speed of the braking, the clamping force, and the initial wear of the pads.

Figures 3 and 4 graphically present the relation of pad wear and the initial speed with a proposal of an approximating function. For the square, power and exponential functions, the authors verified the fitment of the test stand results to the regression model based on the coefficient of determination R^2 . The values of the coefficients for individual regression functions have been included in the graphs (in Figs. 3 and 4).

When analyzing the results presented in Figure 3 and Figure 4, the authors have concluded that irrespective of the clamping force applied to the disc, mass to be decelerated and pad thickness, the mass wear as a function of speed, at which the deceleration initiated, it is possible to model utilizing a regression square function. In each case, the authors obtained the highest coefficient of determination in the range 0.98-0.99.

Figure 5, for selected braking combinations, presents the mass wear of the pads as a function of speed, at which the braking starts and pad thickness for a given clamping force and mass to be decelerated.

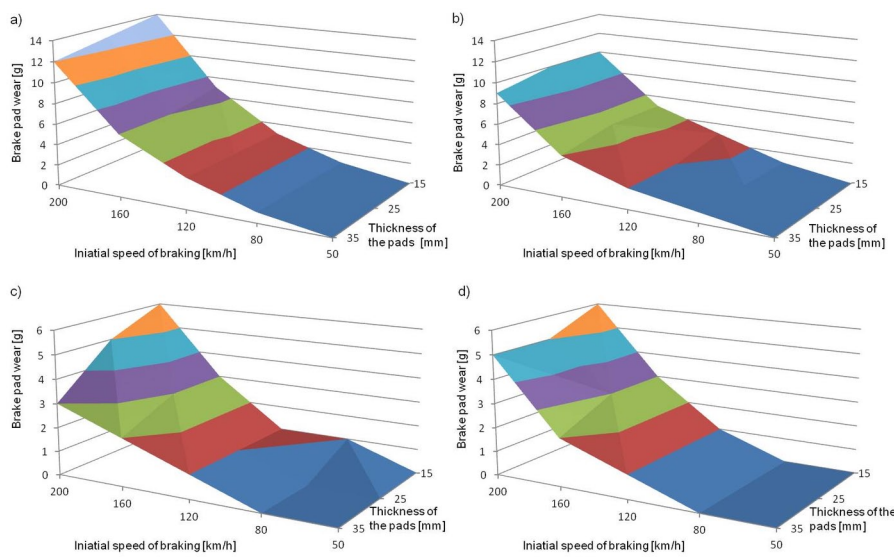


Fig. 5. Mass wear of the pads at: a) $N=40$ kN, $M_h=6.7$ t, b) $N=28$ kN, $M_h=6.7$ t, c) $N=16$ kN, $M_h=4.7$ t, d) $N=26$ kN, $M_h=4.7$ t

The test stand investigations carried out in the number of 150 braking instances at different combinations of speed, clamping force, mass to be decelerated, and pad thickness confirm the relation (strong relation, a square function that can be modeled) between the mass wear of the brake pads and the input (preset) brake parameters.

5. Modelling of brake pad mass wear

Based on the results of the brake pad mass wear investigations, the authors attempted to model this wear based on the following input parameters: contact surface area of the brake pads with the disc, brake pad thickness, clamping force of the pad against the brake disc, rail vehicle mass to be decelerated per single brake disc and the speed at which the braking initiates.

For modeling of the brake pad mass wear, a multiple regression model was applied, otherwise referred to as multinomial regression. This is a method in which the value of random variable Y depends on the k -th independent quantity (X_1, X_2, \dots, X_k). Based on a given sample of results, according to [13], the authors determined the invariable parameters $\beta_0, \beta_1, \dots, \beta_k$ utilizing the least squares. For the determina-

tion of the mass wear of the brake pads, the following relation was proposed:

$$g_w = \beta_1 P_O + \beta_2 G_O + \beta_3 N + \beta_4 M_h + \beta_5 v + \beta_6 v^2 + \beta_0 \quad [g] \quad (1)$$

where: P_O - the contact surface area of the pad with the disc (4×175 cm², 4×200 cm²); G_O - thickness of the pads (new $G_1=35$ mm, worn to $G_2=25$ mm and $G_3=15$ mm); N - clamping force of the pad against the disc ($N=16, 25, 26, 28, 36, 40$ and 44 kN); M_h - mass to be decelerated per single disc ($M_h=4.4; 4.7; 5.7; 6.7$ and 7.5 t); v - initial speed of braking ($v=50, 80, 120, 160$ and 200 km/h).

The multiple regression for model (1) were calculated according to relation (2) [23].

$$r = \frac{\sum_{i=1}^n (x_i - \bar{x})(y_i - \bar{y})}{\sqrt{\sum_{i=1}^n (x_i - \bar{x})^2 \sum_{i=1}^n (y_i - \bar{y})^2}} \quad (2)$$

where: x - average values of quantity x and quantity y ; y_i, x_i - descriptive variables.

At the same time, the authors introduced a validation of the empirical model described with relation (3) and the significance of the system of individual coefficients of regression was verified. When validating the empirical model described with formulae (3) and (4), statistical tests were performed. Based on the example of mass wear, the statistical hypothesis related to the significance of the system of coefficients of regression was formulated as follows.

$$H_0 : \sum_{k=0}^n \beta_k^2 = 0; (k=0, 1, 2, \dots, 6) \quad (3)$$

$$H_1 : \sum_{k=0}^n \beta_k^2 \neq 0; (k=0, 1, 2, \dots, 6) \quad (4)$$

Rejecting H_0 , h_e denoted that there are statistical grounds to assume a linear relation between the dependent and at least one explanatory variable. In the regression model significance test, the F Snedecor distribution was applied.

For the determination of the the significance of individual coefficients of regression, hypotheses described with the following relations were formed:

$$H_0 : \beta_k = 0; \quad (5)$$

$$H_1 : \beta_k \neq 0. \quad (6)$$

For testing of hypotheses related to the significance of individual regression coefficients, a t-Student distribution was applied. If significance F is lower than the assumed level of significance α ($\alpha=0.05$), there are grounds to reject the zero hypothesis and adopt the fact that there exists a linear relation between the dependent variable and all explanatory variables.

Table 2. Results of the statistical test for the pad wear model of a disc brake

Coefficient	Value	Value F^*
β_1	$-2.11 \cdot 10^{-2}$	0.24
β_2	$-3.40 \cdot 10^{-2}$	0.12
β_3	$9.12 \cdot 10^{-2}$	$4.56 \cdot 10^{-5}$
β_4	$1.17 \cdot 10^{-4}$	$2.15 \cdot 10^{-11}$
β_5	$-4.94 \cdot 10^{-2}$	$1.32 \cdot 10^{-2}$
β_6	$4.86 \cdot 10^{-4}$	$4.16 \cdot 10^{-9}$
β_0	-3.22	0.39
R^2	0.81	-
F^{**}	$6.31 \cdot 10^{-49}$	

* significance for individual coefficients of regression
 ** significance for the entire system

The values of the multiple regression function coefficients along with the coefficient of determination R^2 for the pad mass wear model after performing the statistical tests are presented in Table 2.

When analyzing the results of the statistical test contained in Table 2, the authors observed that some of the coefficients (β_0 , β_1 and β_2) of the model described with formula (1) do not meet the assumed level of significance $\alpha=0.05$. The said coefficients were removed and the multinomial regression was determined anew, excluding the variables related to the contact surface area of the pad with the disc (P_o) and the thickness of the pads (G_o). The results of the statistical test for the pad wear model after validation of its coefficients are presented in Table 3.

Table 4. Correlation matrix for the model of mass wear variables

Variable	Clamping force N	Vehicle mass to be decelerated M_h	Speed v	Square speed v^2	Coefficient of correlation
Clamping force N	1	0.29	0	0	0.24
Vehicle mass to be decelerated M_h	0.29	1	$3.75 \cdot 10^{-17}$	$9.09 \cdot 10^{-18}$	0.32
Speed v	0	$3.75 \cdot 10^{-17}$	1	0.98	0.78
Square speed v^2	0	$9.09 \cdot 10^{-18}$	0.98	1	0.81
Coefficient of correlation	0.24	0.32	0.78	0.81	1.0

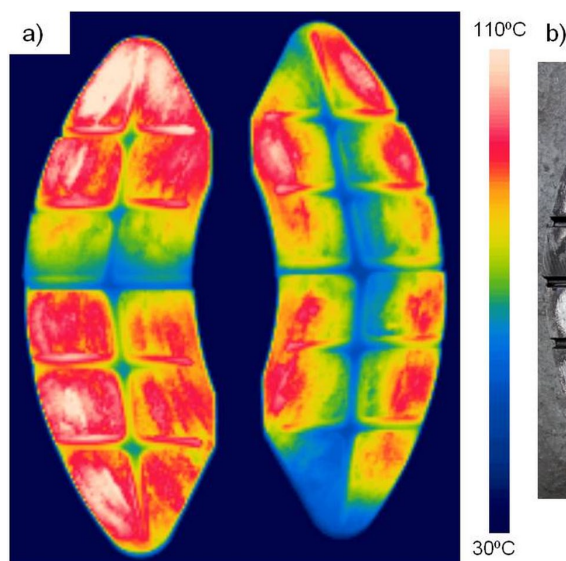


Fig. 6. View of the set of brake pads after: a) thermographic examination, b) friction-mechanical tests after braking from the speed of 120 km/h

Table 3. Results of the statistical test for the brake pad wear model of a disc brake after validation of its coefficients

Coefficient	Value	Value F^*
β_1	$9.00 \cdot 10^{-2}$	$6.09 \cdot 10^{-5}$
β_2	1.16	$3.04 \cdot 10^{-11}$
β_3	$-4.94 \cdot 10^{-2}$	$1.37 \cdot 10^{-2}$
β_4	$4.86 \cdot 10^{-4}$	$2.15 \cdot 10^{-11}$
β_0	-8.11	$4.89 \cdot 10^{-9}$
R^2	0.80	-
F^{**}	$2.67 \cdot 10^{-50}$	

* significance for individual coefficients of regression
 ** significance for the entire system

The final form of the mass wear based on the preset quantities describing the braking process upon validation of the parameters of the multiple regression model is presented by the relationship:

$$g_w = 9.00 \cdot 10^{-2} N + 1.16 M_h - 4.94 \cdot 10^{-2} v + 4.86 \cdot 10^{-4} v^2 - 8.11 \quad [g] \quad (7)$$

Then, the Pearson coefficient of linear correlation (Table 4) was validated for the analysed variables (clamping force of the brake pads, mass to be decelerated, and the speed, at which the braking initiates) upon validation of the coefficients of the brake pad mass wear model.

When analysing the values of the coefficient of correlation in Table 4, the Authors observed that changes in the pad mass wear were most significantly influenced by braking speed of the onset of brak-

ing ($r=0.81$), which confirms a strong dependence of g_w on v . The clamping force N of the pads and the mass M_h to be decelerated have an insignificant impact on the changes of g_w . The coefficient of correlation in the case of these variables falls in the range of 0.2-0.4.

The thermographic investigations carried out parallel to the friction-mechanical ones have shown the uneven contact surface area between the pads and the disc, as shown in Fig. 6. After each braking, the pads were removed and a thermographic image was recorded in order to determine the temperature distribution on the brake pads.

The regression model described with Formula (7) refers to determining the mass wear of the set of brake pads (4 pcs.) after a single braking from the preset speed. Thermographic examinations have proven that the temperature of the friction elements of the pads is not the same throughout their entire surface. The maximum temperature was $+109^\circ\text{C}$ in the upper section of the left brake pad, while the lowest recorded temperature of the brake pad was $+62^\circ\text{C}$ in the lower section of the right

brake pad. The problem of uneven distribution of braking forces was attributed by Sawczuk et al. [36] to changes in the geometry of the lever system and an uneven distribution of the masses on the left and right sides of the level system.

By analyzing the results of the friction pad weight wear of the friction pads after 150 brake applications, in relation to the proposed mass wear model described by the relationship (7), a good and satisfactory precision of the model in relation to the results of research. It was established on the basis of the coefficient of determination for the entire model, taking into account all variables after their verification (Table 3). The determination coefficient for the model was 0.80.

8. Conclusions

In the paper, the authors presented the results of investigations of the mass wear of brake pads on a certified test stand for testing disc brakes of rail-vehicles. Based on the friction-mechanical tests, after 150 instances of braking with different combinations of such parameters as, inter alia, clamping force, speed, or vehicle mass to be decelerated, a regression model was made of the mass wear (expressed in grams) of the brake pads after each instance of braking.

Based on the investigations performed and modelling of the brake pad wear the following have been confirmed:

1. Of the braking process parameters, the most significant impact on brake pad increase in the mass wear is the initial speed of the deceleration with the coefficient of great correlation of the regression model $r=0.80$ and the vehicle mass to be decelerated with the small coefficient of correlation $r=0.32$.

2. The clamping force of the pads against the brake disc has a small influence on the mass wear of the brake pads with the minor coefficient of correlation $r=0.24$.
3. Such parameters of the process as the contact surface area of the pad with the disc and its wear, as defined by the measurement of its thickness, do not influence the regression model, and thus have no impact on the increase in the pad mass wear.
4. Based on data from the vehicle's driving route, the number of brakes and stops, the brake wear model of the pads allows the calculation of the particulate matter (PM) emitted into the environment from the friction material on the basis of a single braking.
5. Observation of the surfaces of the friction pads after each instance of braking using a thermographic camera has proven an uneven distribution of forces applied to the brake pads, as has already been discussed in other authors' works, e.g. [36].

In further work, in order to model the wear of brake pads, the authors plan to include more variables from the group of parameters related to the braking process such as perforation of the brake disc. This type of brake disc is often used in motor vehicles and, despite the improved contact of the pads with the disc, a significant increase in the wear of the brake pads is still possible.

Acknowledgment

The investigations were carried out within the Implementation Doctorate Program of the Ministry of Education and Science realized in the years 2021-2025.

References

1. Abbasi S, Wahlströma J, Olander L, Larsson C, Olofssona U, Sellgren U. A study of airborne wear particles generated from organic railway brake pads and brake discs. *Wear* 2011; 273: 93-99, <https://doi.org/10.1016/j.wear.2011.04.013>.
2. Ahmadijokan F, Shojaei A, Dordanihaghghi S, Jafarpour E, Mohammadi S, Arjmand M. Effects of hybrid carbon-aramid fiber on performance of non-asbestos organic brake friction composite. *Wear* 2020; 452-453: 203280, <https://doi.org/10.1016/j.wear.2020.203280>.
3. Amaren SG, Yawas DS, Aku SY. Effect of periwinkles shell particle size on the wear behavior of asbestos free brake pad. *Results in Physics* 2013; 3: 109-114, <https://doi.org/10.1016/j.rinp.2013.06.004>.
4. Anoop S, Natarajan S, Kumaresh Babu SP. Analysis of factors influencing dry sliding wear behavior of Al/SiCp-brake pad tribosystem. *Materials and Design* 2009; 30: 3831-3838, <https://doi.org/10.1016/j.matdes.2009.03.034>.
5. Bernstein DM, Toth B, Rogers RA, Kunzendorf P, Phillips JI, Schaudien DS. Final results from a 90-day quantitative inhalation toxicology study evaluating the dose-response and fate in the lung and pleura of chrysotile-containing brake dust compared to TiO₂, chrysotile, crocidolite or amosite asbestos: Histopathological examination, confocal microscopy and collagen quantification of the lung and pleural cavity. *Toxicology and Applied Pharmacology* 2021; 424: 115598, <https://doi.org/10.1016/j.taap.2021.115598>.
6. Bernstein DM, Toth B, Rogers RA, Kling DE, Kunzendorf P, Phillips JI, Ernst H. Evaluation of the exposure, dose-response and fate in the lung and pleura of chrysotile-containing brake dust compared to TiO₂, chrysotile, crocidolite or amosite asbestos in a 90-day quantitative inhalation toxicology study –Interim results Part 1: Experimental design, aerosol exposure, lung burdens and BAL. *Toxicology and Applied Pharmacology* 2020; 387: 114856, <https://doi.org/10.1016/j.taap.2019.114856>.
7. Chandradass J, Baskara Sethupathi P, Amutha Surabi M. Fabrication and characterization of asbestos free epoxy based brake pads using carbon fiber as reinforcement. *Materials Today: Proceedings* 2021; 45: 7222-7227, <https://doi.org/10.1016/j.matpr.2021.02.530>.
8. Chandradass J, Amutha Surabi M, Baskara Sethupathi P, Jawahar P. Development of low cost brake pad material using asbestos free sugarcane bagasse ash hybrid composites. *Materials Today: Proceedings* 2021; 45: 7050-7057, <https://doi.org/10.1016/j.matpr.2021.01.877>.
9. Chen F, Li Z, Luo Y, Li D, Ma W, Zhang C, Tang H, Li F, Xiao P. Braking behaviors of Cu-based PM brake pads mating with C/C–SiC and 30CrMnSi steel discs under high-energy braking. *Wear* 2021; 486-487: 204019, <https://doi.org/10.1016/j.wear.2021.204019>.
10. Chen J, Hu H, Ge Y, Wang K, Huang W, He Z. An Energy Storage System for Recycling Regenerative Braking Energy in High-Speed Railway. *IEEE Transactions on Power Delivery* 2020; 36(1): 320-330, DOI: 10.1109/TPWRD.2020.2980018.
11. El-Tayeb NSM, Liew KW. Effect of water spray on friction and wear behaviour of noncommercial and commercial brake pad materials. *Journal of Materials Processing Technology* 2008; 208: 135-144, <https://doi.org/10.1016/j.jmatprotec.2007.12.111>.
12. Elzayady N, Elsoeudy R. Microstructure and wear mechanisms investigation on the brake pad. *Journal of Materials Research and Technology* 2021; 11: 2314-2335, <https://doi.org/10.1016/j.jmrt.2021.02.045>.
13. Gajek K, Kałuszka M. Wnioskowanie statystyczne – modele i metody. WNT, Warszawa 2000: 90-95.
14. Glišović J, Pešić R, Lukić J, Miloradović D. Airborne wear particles from automotive brake system: environmental and health issues. 1st International conference on Quality of Life. June 2016: 289-295.
15. Głowacz A, Tadeusiewicz R, Legutko S, Caesarendra W, Irfan M, Liu H, Brumercik F, Gutten M, Sulowicz M, Daviu JA, et al. Fault diagnosis of angle grinders and electric impact drills using acoustic signals. *Applied Acoustics* 2021; 179: 108070, <https://doi.org/10.1016/j.apacoust.2021.108070>.

16. Gurunath PV, Bijwe J. Friction and wear studies on brake-pad materials based on newly developed resin. *Wear* 2007; 263: 1212-1219, <https://doi.org/10.1016/j.wear.2006.12.050>.
17. Hatam A, Khalkhali A. Simulation and sensitivity analysis of wear on the automotive brake pad. *Simulation Modelling Practice and Theory* 2018; 84: 106-123, <https://doi.org/10.1016/j.simpat.2018.01.009>.
18. Idris UD, Aigbodion VS, Akubakar IJ, Nwoye CI. Eco-friendly asbestos free brake-pad: Using banana peels. *Journal of King Saud University – Engineering Sciences* 2015; 27: 185-192, <https://doi.org/10.1016/j.jksues.2013.06.006>.
19. Ingo GM, D'Uffizi M, Falso G, Bultrini G, Padeletti G. Thermal and microchemical investigation of automotive brake pad wear residues. *Thermochimica Acta* 2004; 418: 61-68, <https://doi.org/10.1016/j.tca.2003.11.042>.
20. Jacob Moses A, Suresh Babu A, Ananda Kumar S. Analysis of physical properties and wear behavior of phenol formaldehyde – Basalt fiber reinforced brake pad. *Materials Today: Proceedings* 2020; 33: 1128-1132, <https://doi.org/10.1016/j.matpr.2020.07.228>.
21. Jiang L, Jiang YL, Yu L, Yang HL, Li ZS, Ding YD, Fu GF. Fabrication, microstructure, friction and wear properties of SiC3D/Al brake disc-graphite/SiC pad tribo-couple for high-speed train. *Transactions of Nonferrous Metals Society of China* 2019; 29: 1889-1902, [https://doi.org/10.1016/S1003-6326\(19\)65097-1](https://doi.org/10.1016/S1003-6326(19)65097-1).
22. Kalel N, Bhatt B, Darpe A, Bijwe J. Argon low-pressure plasma treatment to stainless steel particles to augment the wear resistance of Cu-free brake-pads. *Tribology International* 2022; 167: 107366, <https://doi.org/10.1016/j.triboint.2021.107366>.
23. Kryszicki W, Włodarski L. *Analiza matematyczna w zadaniach*, Wydawnictwo PWN, Warszawa 2007: 412-426.
24. Laguna-Camacho JR, Juárez-Morales G, Calderón-Ramón C, Velázquez-Martínez V, Hernández-Romero I, Méndez-Méndez JV, Vite-Torres M. A study of the wear mechanisms of disk and shoe brake pads. *Engineering Failure Analysis* 2015; 56: 348-359, <https://doi.org/10.1016/j.engfailanal.2015.01.004>.
25. Mahale V, Bijwe J. Exploration of plasma treated stainless steel swarf to reduce the wear of copper-free brake-pads. *Tribology International* 2020; 144: 106111, <https://doi.org/10.1016/j.triboint.2019.106111>.
26. Maiorana S, Teoldi F, Silvani S, Mancini A, Sanguineti A, Mariani F, Cella C, Lopez A, Potenza MAC, Lodi M, Dupin D, Sanvito T, Bonfanti A, Benfenati E, Baderna D. Phytotoxicity of wear debris from traditional and innovative brake pads. *Environment International* 2019; 123: 156-163, <https://doi.org/10.1016/j.envint.2018.11.057>.
27. Park J, Joo B, Seo H, Song W, Lee JJ, Lee WK, Jang H. Analysis of wear induced particle emissions from brake pads during the worldwide harmonized light vehicles test procedure (WLTP). *Wear* 2021; 466-467: 203539, <https://doi.org/10.1016/j.wear.2020.203539>.
28. Pinca-Bretotean C, Josan A, Putan V. Testing of brake pads made of non asbestos organic friction composite on specialized station. *Materials Today: Proceedings* 2021; 45: 4183-4188, <https://doi.org/10.1016/j.matpr.2020.12.039>.
29. Polajnar M, Kalin M, Thorbjörnsson I, Thorgrímsson JT, Valle N, Botor-Probiez A. Friction and wear performance of functionally graded ductile iron for brake pads. *Wear* 2017; 382-383: 85-94, <https://doi.org/10.1016/j.wear.2017.04.015>.
30. Pujari S, Srikanth S. Experimental investigations on wear properties of Palm kernel reinforced composites for brake pad applications. *Defence Technology* 2019; 15: 295-299, <https://doi.org/10.1016/j.dt.2018.11.006>.
31. Rajambal K, Umamaheswari B, Chellamuthu C. Electrical braking of large wind turbines. *Renewable Energy* 2005; 30: 2235-2245, <https://doi.org/10.1016/j.renene.2004.11.002>.
32. Rakov V, Kapustin A, Danilov I. Study of braking energy recovery impact on cost-efficiency and environmental safety of vehicle. *Transportation Research Procedia* 2020; 50: 559–565, <https://doi.org/10.1016/j.trpro.2020.10.067>.
33. Rymaniak L, Kaminska M, Szymlet N, Grzeszczyk R. Analysis of Harmful Exhaust Gas Concentrations in Cloud behind a Vehicle with a Spark Ignition Engine. *Energies* 2021; 14(6): 1-14, <https://doi.org/10.3390/en14061769>.
34. Sawczuk W. Application of vibroacoustic diagnostics to evaluation of wear of friction pads rail brake disc. *Eksploatacja i Niezawodność - Maintenance and Reliability* 2016; 18(4): 565-571, <http://doi.org/10.17531/ein.2016.4.11>.
35. Sawczuk W, Ulbrich D, Kowalczyk J, Merksisz-Guranowska A. Evaluation of Wear of Disc Brake Friction Linings and the Variability of the Friction Coefficient on the Basis of Vibroacoustic Signals. *Sensors* 2021; 21(17): 5927-1-5927-21, <https://doi.org/10.3390/s21175927>.
36. Sawczuk W, Merksisz-Guranowska A, Rilo Cañas AM. Assessment of disc brake vibration in rail vehicle operation on the basis of brake stand. *Eksploatacja i Niezawodność - Maintenance and Reliability* 2021; 23 (1): 221 – 230, <http://doi.org/10.17531/ein.2021.2.2>.
37. Smoczyński P, Gill A, Kadziński A, Maintenance layers for railway infrastructure in Poland. *Transport* 2020; 35(6): 605-615, <https://doi.org/10.3846/transport.2020.14137>.
38. Söderberg A, Andersson S. Simulation of wear and contact pressure distribution at the pad-to-rotor interface in a disc brake using general purpose finite element analysis software. *Wear* 2009; 267: 2243-2251, <https://doi.org/10.1016/j.wear.2009.09.004>.
39. Świdarski A, Borucka A, Jacyna-Golda I, Szczepański E. Wear of brake system components in various operating conditions of vehicle in the transport company. *Eksploatacja i Niezawodność - Maintenance and Reliability* 2019; 21(1): 1-9, <http://doi.org/10.17531/ein.2019.1.1>.
40. Tavangar R, Moghadam HA, Khavandi A, Banaeifar S. Comparison of dry sliding behavior and wear mechanism of low metallic and copper-free brake pads. *Tribology International* 2020; 151: 106416, <https://doi.org/10.1016/j.triboint.2020.106416>.
41. Thendral Selvam P, Pugazhenthir R, Dhanasekaran C, Chandrasekaran M, Sivaganesan S. Experimental investigation on the frictional wear behaviour of TiAlN coated brake pads. *Materials Today: Proceedings* 2021; 37: 2419-2426, <https://doi.org/10.1016/j.matpr.2020.08.272>.
42. UIC Code 541-3: Brakes – Disc brakes and their application – General conditions for the approval of brake pads. 7th edition, January 2010.
43. UIC Code 541-4: Brakes – Brakes with composite brake blocks – General conditions for the certification of composite brake blocks. 6th edition, November 2020.
44. Urbaniak M, Kardas-Cinal E. Optimization of using recuperative braking energy on a double-track railway line. *Transportation Research Procedia* 2019; 40: 1208–1215, <https://doi.org/10.1016/j.trpro.2019.07.168>.
45. Varazhun I, Shimanovsky A, Zavarotny A. Determination of Longitudinal Forces in the Cars Automatic Couplers as Train Electrodynamic Braking. *Procedia Engineering* 2016; 134: 415-421, <https://doi.org/10.1016/j.proeng.2016.01.032>.
46. Verma PCh, Menapace L, Bonfanti A, Ciudin R, Gialanella S, Straffelini G. Braking pad-disc system: Wear mechanisms and formation of wear fragments. *Wear* 2015; 322-323: 251-258, <https://doi.org/10.1016/j.wear.2014.11.019>.
47. Wahlström J, Gventsadze D, Olander L, Kutelia E, Gventsadze L, Tsurtsumia O, Olofsson U. A pin-on-disc investigation of novel nanoporous composite-based and conventional brake pad materials focussing on airborne wear particles. *Tribology International* 2011; 44: 1838-1843, <https://doi.org/10.1016/j.triboint.2011.07.008>.

48. Xiao JK, Xiao SX, Chen J, Zhang C. Wear mechanism of Cu-based brake pad for high-speed train braking at speed of 380 km/h. *Tribology International* 2020; 150: 106357, <https://doi.org/10.1016/j.triboint.2020.106357>.
49. Yawas DS, Aku SY, Amaren SG. Morphology and properties of periwinkle shell asbestos-free brake pad. *Journal of King Saud University – Engineering Sciences* 2016; 28: 103-109, <https://doi.org/10.1016/j.jksues.2013.11.002>.
50. Yevtushenko AA, Grzes P. Axisymmetric FEA of temperature in a pad/disc brake system at temperature-dependent coefficients of friction and wear. *International Communications in Heat and Mass Transfer* 2012; 39: 1045-1053, <https://doi.org/10.1016/j.icheatmasstransfer.2012.07.025>.
51. Zhang P, Zhang L, Wei D, Wu P, Cao J, Shijia C, Qu X. A high-performance copper-based brake pad for high-speed railway trains and its surface substance evolution and wear mechanism at high temperature. *Wear* 2020; 444-445: 203182, <https://doi.org/10.1016/j.wear.2019.203182>.